Biochemical Pharmacology 81 (2011) 713–722

Contents lists available at ScienceDirect

Biochemical Pharmacology

journal homepage: www.elsevier.com/locate/biochempharm

Effects of hippuristanol, an inhibitor of eIF4A, on adult T-cell leukemia

Tomoyuki Tsumuraya [a,b], Chie Ishikawa [a,c], Yoshiaki Machijima [a], Sawako Nakachi [a,d], Masachika Senba [e], Junichi Tanaka [f], Naoki Mori [a,*]

[a] Department of Microbiology and Oncology, Graduate School of Medicine, University of the Ryukyus, 207 Uehara, Nishihara, Okinawa 903-0215, Japan
[b] Department of Oral and Maxillofacial Functional Rehabilitation, Graduate School of Medicine, University of the Ryukyus, 207 Uehara, Nishihara, Okinawa 903-0215, Japan
[c] Transdisciplinary Research Organization for Subtropics and Island Studies, 1 Senbaru, Nishihara, Okinawa 903-0213, Japan
[d] Department of Endocrinology, Metabolism and Hematology, Graduate School of Medicine, University of the Ryukyus, 207 Uehara, Nishihara, Okinawa 903-0215, Japan
[e] Department of Pathology, Institute of Tropical Medicine, Nagasaki University, 1-12-4 Sakamoto, Nagasaki 852-8523, Japan
[f] Department of Chemistry, Biology and Marine Science, University of the Ryukyus, 1 Senbaru, Nishihara, Okinawa 903-0213, Japan

ARTICLE INFO

Article history:
Received 23 September 2010
Accepted 22 December 2010
Available online 8 January 2011

Keywords:
ATL
Hippuristanol
NF-kappaB
AP-1
eIF4A

ABSTRACT

We evaluated the anti-adult T-cell leukemia (ATL) effects of hippuristanol, an eukaryotic translation initiation inhibitor from the coral *Isis hippuris*. Hippuristanol inhibited proliferation of HTLV-1-infected T-cell lines and ATL cells, but not normal peripheral blood mononuclear cells. It induced cell cycle arrest during G_1 phase by reducing the expression of cyclin D1, cyclin D2, CDK4 and CDK6, and induced apoptosis by reducing the expression of Bcl-x_L, c-IAP2, XIAP and c-FLIP. The induced apoptosis was associated with activation of caspase-3, -8 and -9. Hippuristanol also suppressed IkappaBalpha phosphorylation and depleted IKKalpha, IKKgamma, JunB and JunD, resulting in inactivation of NF-kappaB and AP-1. It also suppressed carbonic anhydrase type II expression. In addition to its *in vitro* effects, hippuristanol suppressed tumor growth in mice with severe combined immunodeficiency harboring tumors induced by inoculation of HTLV-1-infected T cells. These preclinical data suggest that hippuristanol could be a potentially useful therapeutic agent for patients with ATL.

1. Introduction

Human T-cell leukemia virus type 1 (HTLV-1) infection causes adult T-cell leukemia (ATL), a progressively debilitating disease of peripheral $CD4^+$ T cells [1–3]. Despite the development of intensive combination chemotherapy regimens, bone marrow transplantation and monoclonal antibodies, the prognosis of patients with ATL remains poor [4]. The median survival time of patients with aggressive ATL such as acute and lymphoma types, is less than 13 months [5]. This extremely grave outcome is mainly due to intrinsic resistance of leukemic cells to conventional or even high doses of chemotherapy and to severe immunosuppression. Therefore, it is important to find novel therapeutic approaches to prevent the development of ATL and to prolong survival after its occurrence.

The viral Tax protein plays a critical role in the regulation of proliferation and transformation of HTLV-1-infected T cells. Tax does not only transactivate viral genes but also activates cellular transcriptional factors including NF-kappaB and AP-1. NF-kappaB and AP-1 have been implicated recently in cell survival and proliferation pathways. Both pathways are activated in ATL cells that do not express Tax, although the mechanism of activation remains unknown [6,7].

Hippuristanol, a polyoxygenated steroid was discovered in the coral *Isis hippuris*. It was reported previously that this natural product appeared to work through eukaryotic initiation factor (eIF)4A, an ATP-dependent RNA helicase, blocking its binding to mRNA, hence inhibiting translational initiation [8]. Given the critical role of translation in cell proliferation, hipurristanol is considered a promising lead for the development of anti-cancer agents. Furthermore, translation is also necessary for viral infection, suggesting that hippuristanol can be a potentially useful anti-viral agent. Indeed, poliovirus replication is delayed when infected cells are exposed to hippuristanol [8].

It is known that unrestrained proliferation is the most aggressive phenotype of ATL cells and correlates with ATL progression [9]. We hypothesized that hippuristanol can inhibit cell proliferation and viral replication in HTLV-1-infected T cells. The present study was designed to investigate whether hippuristanol is a pharmacologically safe and effective inhibitor of cell growth of HTLV-1-infected T cells. We report here the anti-proliferative effects and molecular mechanisms of the apoptotic effects induced by hippuristanol in HTLV-1-infected T cells. We also report the *in vivo* anti-ATL efficacy in a mouse model.

* Corresponding author. Current address: Department of Internal Medicine, Omoromachi Medical Center, 1-3-1 Uenoya, Naha, Okinawa 900-0011, Japan. Tel.: +81 98 867 2116; fax: +81 98 861 2398.
E-mail address: naokimori50@gmail.com (N. Mori).

0006-2952/$ – see front matter © 2011 Elsevier Inc. All rights reserved.
doi:10.1016/j.bcp.2010.12.025

2. Materials and methods

2.1. Reagents

Hippuristanol was extracted from the gorgonian *I. hippuris* as described previously [8]. Carbonic anhydrase (CA) inhibitor 6-ethoxy-2-benzo-thiazolesulfonamide (ethoxyzolamide) and antibody to IkappaB kinase (IKK)gamma were obtained from Sigma-Aldrich (St. Louis, MO, USA). Antibodies to eIF4AI, carbonic anhydrase type II (CA II), cyclin D2, c-IAP2, IkappaBalpha, JunB, JunD, NF-kappaB subunits p65, p50, c-Rel, p52 and RelB, and AP-1 subunits c-Fos, FosB, Fra-1, Fra-2, c-Jun, JunB and JunD were purchased from Santa Cruz Biotechnology (Santa Cruz, CA, USA). Antibodies to Bax, Bcl-2, CDK4, CDK6 and actin were purchased from NeoMarkers (Fremont, CA, USA). Antibodies to XIAP and cyclin D1 were purchased from Medical & Biological Laboratories (Nagoya, Japan). Antibodies to cleaved poly(ADP-ribose) polymerase (PARP), cleaved caspase-3, cleaved caspase-8, cleaved caspase-9, caspase-9, c-FLIP, survivin, Bak, Akt, IKKalpha, IKKbeta, phospho-IkappaBalpha (Ser32 and Ser36) and Bcl-x_L were purchased from Cell Signaling Technology (Beverly, MA, USA). Antibody to Tax, Lt-4, was described previously [10].

2.2. Cells

The HTLV-1-infected T-cell lines, MT-2 [11], MT-4 [12], HUT-102 [1], MT-1 [13] and ED-40515(−) [14] were cultured in RPMI 1640 medium supplemented with 10% heat-inactivated fetal bovine serum. MT-2 and MT-4 are HTLV-1-transformed T-cell lines, established by an *in vitro* coculture protocol. MT-1 and ED-40515(−) are T-cell lines of leukemic cell origin established from patients with ATL. HUT-102 was also established from a patient with ATL and constitutively expresses viral genes, but its clonal origin is unclear. Peripheral blood mononuclear cells (PBMC) from healthy volunteers and patients with acute type and chronic type ATL were also analyzed. All samples were obtained after informed consent.

2.3. Assays for cell viability and apoptosis

In these assays, 1×10^5/ml (cell lines) or 1×10^6/ml (PBMC) were cultured with various concentrations of hippuristanol or ethoxyzolamide in 96-well plates. After 24 h or 48 h, cell viability was evaluated by measuring the mitochondrial-dependent conversion of the water-soluble tetrazolium (WST)-8 (Wako Pure Chemical Industries, Osaka, Japan) to a colored formazan product. Apoptotic events in cells were detected by staining with phycoerythrin-conjugated Apo2.7 monoclonal antibody (Beckman Coulter, Marseille, France) [15], and analyzed by flow cytometry (Epics XL, Beckman Coulter, Fullerton, CA, USA). For analysis of morphological changes in nuclei, cells were stained by 10 μg/ml Hoechst 33342 (Wako Pure Chemical Industries) and observed under a microscope (model DMI6000, Leica Microsystems, Wetzlar, Germany).

2.4. Cell cycle analysis

Cell cycle analysis was performed with the CycleTEST PLUS DNA reagent kit (Becton Dickinson Immunocytometry Systems, San Jose, CA, USA). Cell suspensions were analyzed on a Coulter EPICS XL using EXPO32 software. The population of cells in each cell cycle phase was determined with MultiCycle software.

2.5. In vitro measurement of caspase activity

Caspase activity was measured using the colorimetric caspase assay kits (Medical & Biological Laboratories). Cell extracts were recovered using the Cell Lysis buffer and assessed for caspase-3, -8 and -9 activities using colorimetric probes. The colorimetric caspase assay kits are based on detection of chromophore *p*-nitroanilide after cleavage from caspase-specific-labeled substrates. Colorimetric readings were performed in an automated microplate reader.

2.6. Western blot analysis

Cells were lysed in a buffer containing 62.5 mM Tris–HCl (pH 6.8), 2% sodium dodecyl sulphate (SDS), 10% glycerol, 6% 2-mercaptoethanol and 0.01% bromophenol blue. Equal amounts of protein (20 μg) were subjected to electrophoresis on SDS-polyacrylamide gels followed by transfer to a polyvinylidene difluoride membrane and probing with the specific antibodies. The bands were visualized with the enhanced chemiluminescence kit (Amersham Biosciences, Piscataway, NJ, USA).

2.7. Reverse transcription-PCR (RT-PCR)

Total cellular RNA was extracted from cells with Trizol (Invitrogen, Carlsbad, CA, USA) according to the protocol provided by the manufacturer. First-strand cDNA was synthesized from 1 μg total cellular RNA using a PrimeScript RT-PCR kit (Takara Bio Inc., Otsu, Japan) with random primers. The primers used were 5′-GAATTGGTGGACGGGCTATTATC-3′ (forward) and 5′-TAGCAC-TATGCTGTTTCGCCTTC-3′ (reverse) for HBZ, 5′-GCTGCAGAACTT-CACTTGGTTCAC-3′ (forward) and 5′-GGCCACGAGGATCGAA-GTTAGTG-3′ (reverse) for CA II, and 5′-GCCAAGGTCATCCATGA-CAACTTTGG-3′ (forward) and 5′-GCCTGCTTCACCACCTTCTT-GATGTC-3′ (reverse) for GAPDH. The program used in semiquantitative RT-PCR for each gene was as follows; 35 cycles for HBZ, 30 cycles for CA II, and 27 cycles for GAPDH. The PCR products were fractionated on 2% agarose gels and visualized by ethidium bromide staining.

2.8. Electrophoretic mobility shift assay (EMSA)

Nuclear extracts were obtained as described by Antalis and Goldbolt [16] with modifications, and EMSA was conducted as described previously [17]. Briefly, 5 μg of nuclear extract was incubated with ^{32}P-labeled probes. The DNA–protein complex was separated from the free oligonucleotides on a 4% polyacrylamide gel. The probes used were prepared by annealing the sense and antisense synthetic oligonucleotides; a typical NF-kappaB element from the IL-2 receptor alpha chain (IL-2Ralpha) gene (5′-gatcCGGCAGGGGAATCTCCCTCTC-3′) and an AP-1 element of the IL-8 gene (5′-gatcGTGATGACTCAGGTT-3′). The oligonucleotide 5′-gatcTGTCGAATGCAAATCACTAGAA-3′, containing the consensus sequence of the octamer binding motif, was used to identify specific binding of the transcription factor Oct-1. This transcription factor regulates the transcription of a number of so-called housekeeping genes. The above underlined sequences represent the NF-kappaB, AP-1 or Oct-1 binding site.

2.9. Detection of NF-kappaB p65

Cells were cultured with or without hippuristanol for 12 h, and then fixed paraformaldehyde for 10 min. For NF-kappaB p65 staining, the cells were permeabilized with 0.1% saponin in phosphate-buffered saline containing 1% bovine serum albumin. The cells were then incubated with a fluorescein isothiocyanate-conjugated rabbit polyclonal antibody for NF-kappaB p65 (Santa Cruz Biotechnology) for 45 min at 4 °C. Protein localization was detected using Leica DMI6000 microscope.

2.10. Intracellular pH measurement

The fluorescent pH sensitive dye, 2′,7′-bis(2-carboxyethyl)-5(6)-carboxyfluorescein-acetoxymethyl ester (BCECF-AM; Dojindo Co., Kumamoto, Japan) was used to measure intracellular pH in HUT-102 cells. BCECF-AM was added to a cell suspension in HEPES buffer to a final concentration of 3 μM. Cells then were incubated at 37 °C for 30 min to allow cellular esterases to hydrolyze the BCECF-AM to the pH sensitive fluorescent molecule BCECF which is negatively charged and relatively impermeable to the plasma membrane. After washing with HEPES buffer three times, cells were analyzed with a flow cytometry. For calibration, loaded cells were incubated in calibration buffer (130 mM KCl, 10 mM NaCl, 1 mM $MgSO_4$ and 10 mM Na-MOPS) with 10 μg/ml nigericin. After 10 min incubation, cells were analyzed with a flow cytometry.

2.11. In vivo therapeutic effect of hippuristanol

Five-week-old female C.B-17/Icr-SCID mice were obtained from Ryukyu Biotec Co. (Urasoe, Japan). Mice were engrafted with 1×10^7 HUT-102 cells by subcutaneous injection in the post-auricular region and then randomly placed into two groups of six mice each, one received the vehicle only, while the other was treated with hippuristanol. Treatment was initiated on the next day of cell inoculation. Hippuristanol was dissolved in 5.2% polyethylene glycol 400 (Wako Pure Chemical Industries) and 5.2% Tween 80 (Becton Dickinson, Franklin Lakes, NJ, USA) at a concentration of 0.25 mg/ml, and 7.5 mg/kg body weight of hippuristanol was administered intraperitoneally every day for 28 days. Control mice received the same volume of the vehicle only for 28 days. The tumor size was monitored once a week. All mice were sacrificed on day 28, and then the tumors were dissected out and their weight was measured. Tumors were also fixed for paraffin embedding and tissue sectioning, and were evaluated using hematoxylin and eosin (HE) for conventional histological assessment. Analysis of DNA fragmentation by fluorescent terminal deoxynucleotidyl transferase-mediated dUTP nick end labelling (TUNEL) was performed using a commercial kit (Roche Applied Science, Mannheim, Germany). In brief, tumor specimens obtained from xenograft models were fixed in 10% neutral buffer formalin and embedded in paraffin. Sections of 3.5 mm were placed on silane-coated glass slides. TUNEL reaction mixture was added, and then anti-fluorescein of horse-radish peroxidase was added. Finally, diamino benzidine substrate (Roche Applied Science) with cobalt chloride and nickel chloride was used. This experiment was performed according to the Guidelines for the Animal Experimentation of the University of the Ryukyus and was approved by the Animal Care and Use Committee of the University of the Ryukyus.

2.12. Statistical analysis

Data were expressed as mean ± SD. Statistical analyses were carried out by the Mann–Whitney *U*-test and Student's *t*-test as appropriate. A *p* value less than 5% denoted the presence of statistical significance.

3. Results

3.1. eIF4A expression in HTLV-1-infected T-cell lines

First, we examined the expression of eIF4A in various HTLV-1-infected T-cell lines (Fig. 1A). HTLV-1-transformed T-cell lines (MT-2 and MT-4) and HUT-102 cells expressed high levels of Tax protein, whereas ATL-derived T-cell lines, MT-1 and ED-40515(−) cells, did not. Compared with normal PBMC, HTLV-1-infected T-cell lines consistently expressed eIF4A protein independent of Tax expression.

3.2. Hippuristanol reduces cell viability of HTLV-1-infected T-cell lines and primary ATL cells

Next, we examined the effect of hippuristanol on cell viability of HTLV-1-infected T-cell lines and primary ATL cells. The addition of hippuristanol at various concentrations to 48-h cultures of various HTLV-1-infected T cells reduced their viability in a dose-dependent

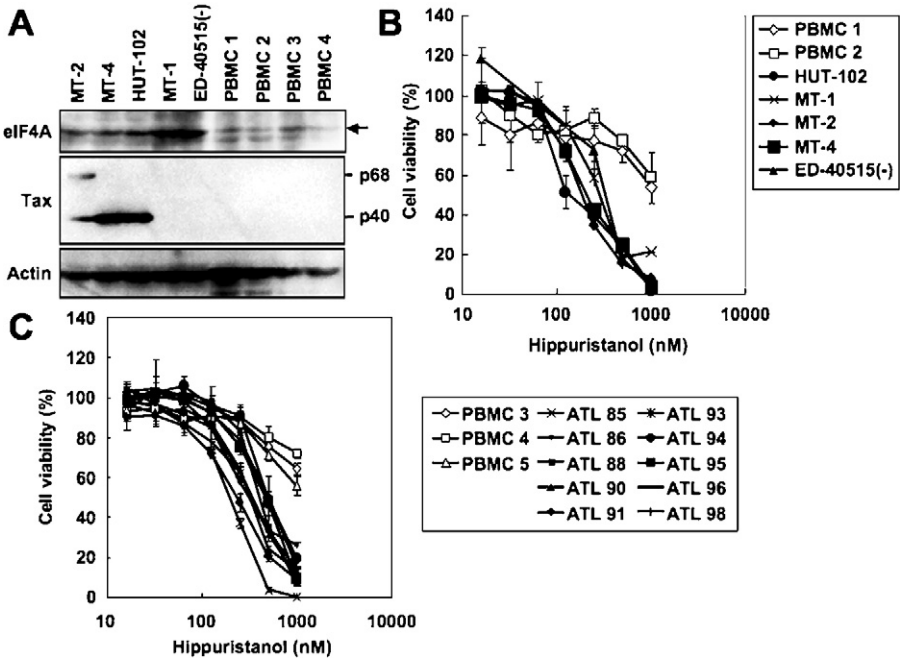

Fig. 1. Hippuristanol reduces cell viability of HTLV-1-infected T-cell lines and PBMC from ATL patients. (A) eIF4A is consistently expressed in HTLV-1-infected T-cell lines. Western blot analysis was carried out for eIF4A, Tax and actin (loading control). HTLV-1-infected T-cell lines (B), PBMC from ATL patients (C) and healthy controls (B and C) were cultured with the indicated concentrations of hippuristanol for 48 h (B) and 24 h (C), and cell viability was determined in triplicate cultures by WST-8 assay. The results are expressed as percentage of control and represent mean ± SD of the results obtained.

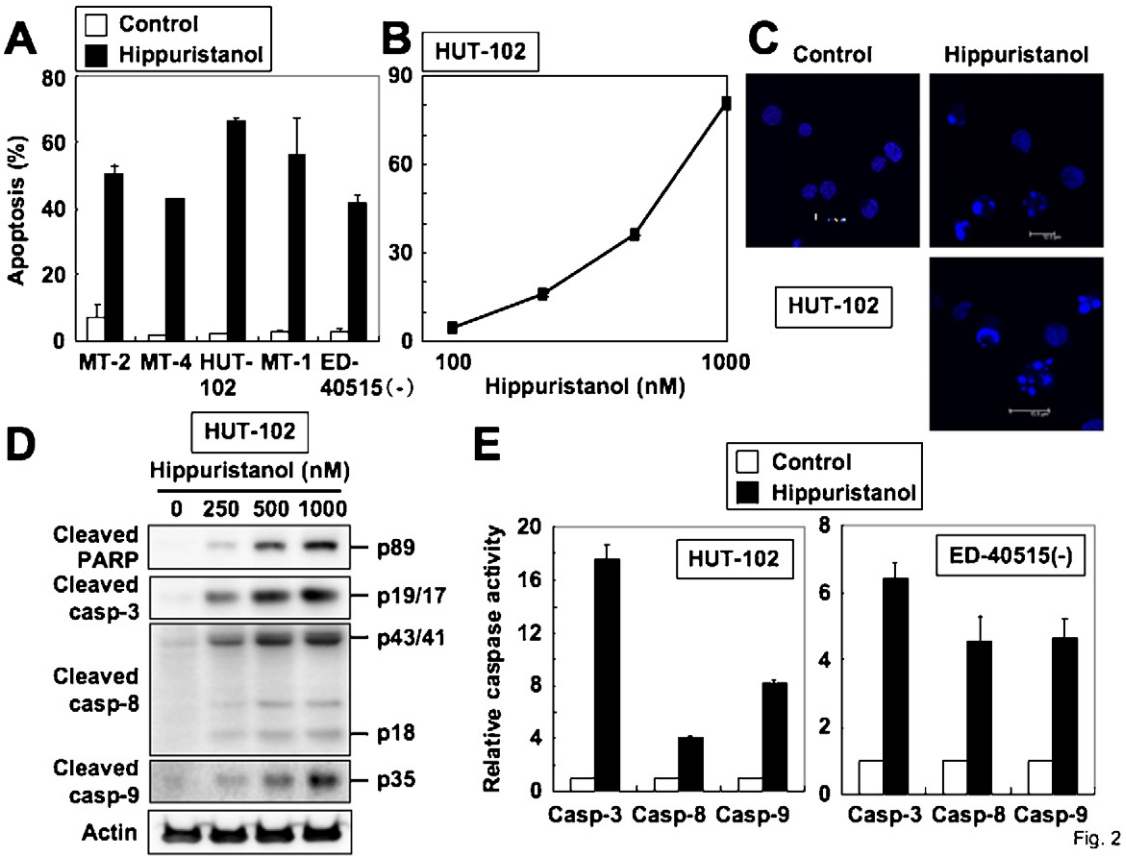

Fig. 2. Hippuristanol induces apoptosis of HTLV-1-infected T-cell lines. (A) HTLV-1-infected T-cell lines were cultured in the absence or presence of 1000 nM hippuristanol. After 48 h, Apo2.7 staining was analyzed by flow cytometry. Data are mean ± SD percentages of apoptotic cells for both untreated and hippuristanol-treated cells ($n = 3$). (B) HUT-102 cells were treated with the indicated concentrations of hippuristanol for 48 h and subjected to Apo2.7 staining. Data are mean ± SD percentages of apoptotic cells ($n = 3$). (C) Hoechst 33342 staining. HUT-102 cells were treated with or without 1000 nM hippuristanol for 24 h and stained by Hoechst 33342. Original magnification, 1000×. (D) HUT-102 cells were incubated with the indicated concentrations of hippuristanol for 24 h. Cellular proteins were resolved by SDS/polyacrylamide gel electrophoresis, and caspase activity was detected by cleavage of PARP, caspase-3, -8 and -9 using immunoblot analysis. Actin was used as a protein-loading control. (E) Hippuristanol-induced apoptosis is caspase-dependent. HUT-102 cells were treated with or without 1000 nM hippuristanol. After 24 h, cell lysates were prepared and incubated with the labeled caspase substrates, and caspase activity was measured using an automated microplate reader. Caspase activity is expressed relative to untreated cells, which were assigned a value of 1. Data are mean ± SD ($n = 3$).

manner, as assessed by WST-8 assay (Fig. 1B), with IC_{50} values (the concentration of hippuristanol required to inhibit cell viability of HTLV-1-infected T-cell lines by 50%) ranging from 189 to 329 nM. Importantly, normal PBMC were resistant to hippuristanol (Fig. 1B and C). We also examined the effects of hippuristanol on freshly isolated ATL cells from 8 patients with acute ATL and 2 with chronic ATL. Treatment of these ATL cells with hippuristanol reduced cell survival compared with PBMC from normal healthy volunteers (Fig. 1C).

3.3. Hippuristanol induces apoptosis of HTLV-1-infected T-cell lines

To investigate the mechanisms by which hippuristanol reduced the cell viability of HTLV-1-infected T-cell lines, we analyzed the frequency of apoptotic cells by immunostaining with Apo2.7, which specifically detects the 38 kDa mitochondrial membrane antigen 7A6 expressed on the mitochondrial outer membrane during apoptosis [15]. Treatment with 1000 nM hippuristanol for 48 h increased the proportion of cells positive for 7A6 among all HTLV-1-infected T-cell lines (Fig. 2A). A significant increase in the apoptotic population was detected in HUT-102 cells in a dose-dependent manner (Fig. 2A and B). A similar experiment was also performed with Hoechst 33342 staining (Fig. 2C). Consistent with the above results, hippuristanol significantly increased chromatin condensation and nuclear fragmentation in HUT-102 cells. Taken together, these results indicate that the inhibitory effect of hippuristanol on the viability of HTLV-1-infected T-cells is mediated through the induction of apoptosis.

3.4. Hippuristanol-induced apoptosis is caspase-dependent

We then investigated whether the observed apoptosis was due to caspase activation. Cell extracts were obtained after various treatments and processed for immunoblot analysis. As shown in Fig. 2D, immunoblot analysis clearly demonstrated the production of cleaved products of the caspase-3-specific substrate PARP, caspase-3, -8 and -9 by hippuristanol in a dose-dependent manner. Immunoblotting allowed the examination of caspases processing, but did not indicate whether the cleavage products were enzymatically active. Therefore, caspase-3, -8 and -9 activities were determined by cleavage of caspase-specific-labeled substrates in colorimetric assays. Hippuristanol resulted in activation of caspases-3, -8 and -9 in HUT-102 and ED-40515(−) cells (Fig. 2E), confirming that hippuristanol-induced apoptosis of HTLV-1-infected T-cell lines is mediated through caspase activation.

3.5. Hippuristanol causes G_1 cell cycle arrest

In the next step, we examined the cellular DNA contents distribution by flow cytometric analysis on cell treatment. Cultivation of HTLV-1-infected T-cells with hippuristanol increased the population of cells in the G_1 phase, with marked reduction of cells in the S phase, relative to untreated cells (Fig. 3). These changes were primarily the result of a G_1 cell cycle arrest in HTLV-1-infected T-cell lines.

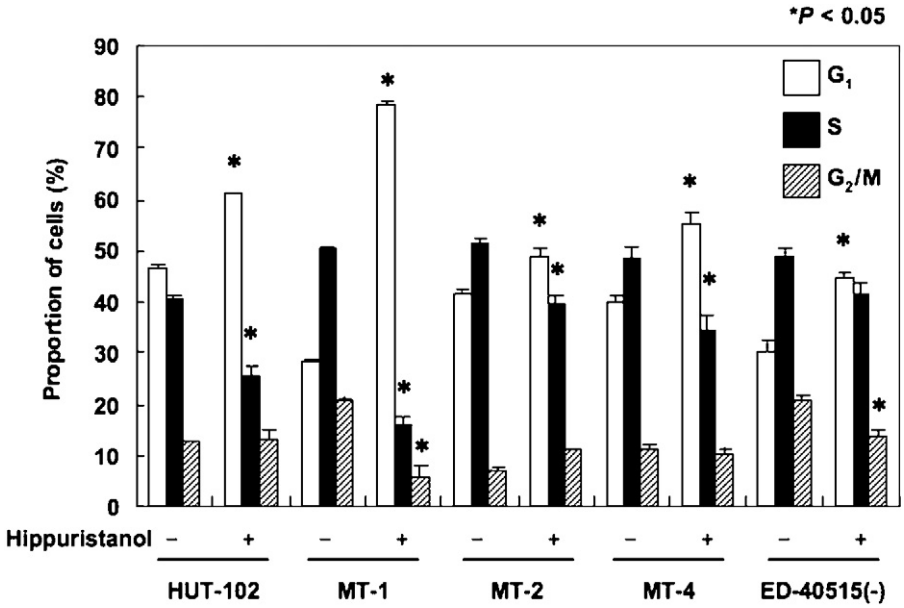

Fig. 3. Hippuristanol induces G_1 cell cycle arrest in HTLV-1-infected T-cell lines. Cells were incubated with or without 1000 nM hippuristanol for 12 h. Cell cycle distribution was analyzed by flow cytometry by staining with propidium iodide. Data are mean ± SD percentage of cells at various phases of the cell cycle ($n = 3$). $^*p < 0.05$ compared with the control.

3.6. *Effects of hippuristanol on expression of cell cycle and apoptosis regulatory proteins and viral Tax and HBZ*

To clarify the molecular mechanisms of hippuristanol-induced inhibition of cell growth and apoptosis, we investigated the effects of hippuristanol on the expression of several intracellular regulators of cell cycle and apoptosis by Western blot analysis. As shown in Fig. 4A, hippuristanol neither altered the expression levels of anti-apoptotic proteins Bcl-2 and survivin, nor those of pro-apoptotic proteins Bax and Bak. In contrast, hippuristanol

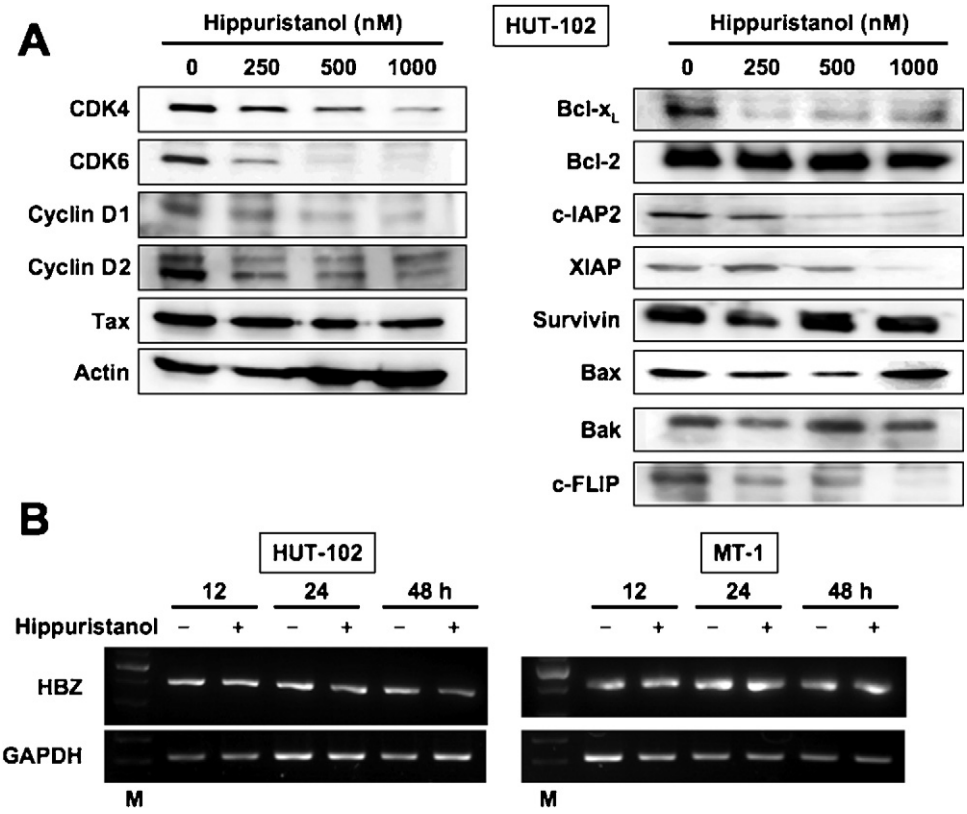

Fig. 4. Effects of hippuristanol on the expression of cell cycle and apoptosis regulatory proteins, and viral Tax protein and HBZ mRNA. (A) HUT-102 cells were treated with various concentrations of hippuristanol for 24 h. Whole cell extracts were prepared and immunoblotted with specific antibodies against cell cycle and apoptosis regulatory proteins. (B) HUT-102 and MT-1 cells were treated with or without 1000 nM hippuristanol for the indicated time periods. HBZ mRNA expression was examined by RT-PCR. Lane M, molecular mass marker.

significantly reduced the expression of cell cycle regulatory proteins cyclin D1, cyclin D2, CDK4 and CDK6, and anti-apoptotic proteins Bcl-x_L, c-IAP2, XIAP and c-FLIP in HUT-102 cells in a dose-dependent manner. Comparable loading of protein was confirmed with a specific antibody for the housekeeping gene product actin (Fig. 4A). Because cyclin D1, cyclin D2, CDK4, CDK6, Bcl-x_L, c-IAP2, XIAP and c-FLIP are Tax-responsive genes [18–24], we also determined the level of Tax expression. However, hippuristanol did not change the protein level of Tax in HUT-102 cells (Fig. 4A). These results indicate that the altered expression levels of cyclin D1, cyclin D2, CDK4, CDK6, Bcl-x_L, c-IAP2, XIAP and c-FLIP proteins did not result from Tax down-regulation.

HTLV-1 basic leucine-zipper (bZIP) factor, HBZ, is encoded on the antisense strand of proviral DNA, and plays a role in the transformation of infected cells into malignant cells [25]. We also examined the level of HBZ mRNA expression, but hippuristanol failed to inhibit its expression level in HUT-102 and MT-1 cells (Fig. 4B).

3.7. Inhibitory effects of hippuristanol on NF-kappaB activation

Several studies have suggested that NF-kappaB can prevent apoptosis and caspase activation as a survival factor and is required for the proliferation of various tumor cell types [26]. Because NF-kappaB is constitutively active in Tax-expressing and HTLV-1-infected T-cell lines as well as primary ATL cells [7], and Tax stimulates the expression of cyclin D2, CDK4, CDK6, Bcl-x_L, c-IAP2, XIAP and c-FLIP through the NF-kappaB pathway [18–23], we examined whether hippuristanol inhibits the NF-kappaB pathway. To study the DNA-binding activity of NF-kappaB, we performed EMSA with radiolabeled double-stranded NF-kappaB oligonucleotides and nuclear extracts from untreated or hippuristanol-treated

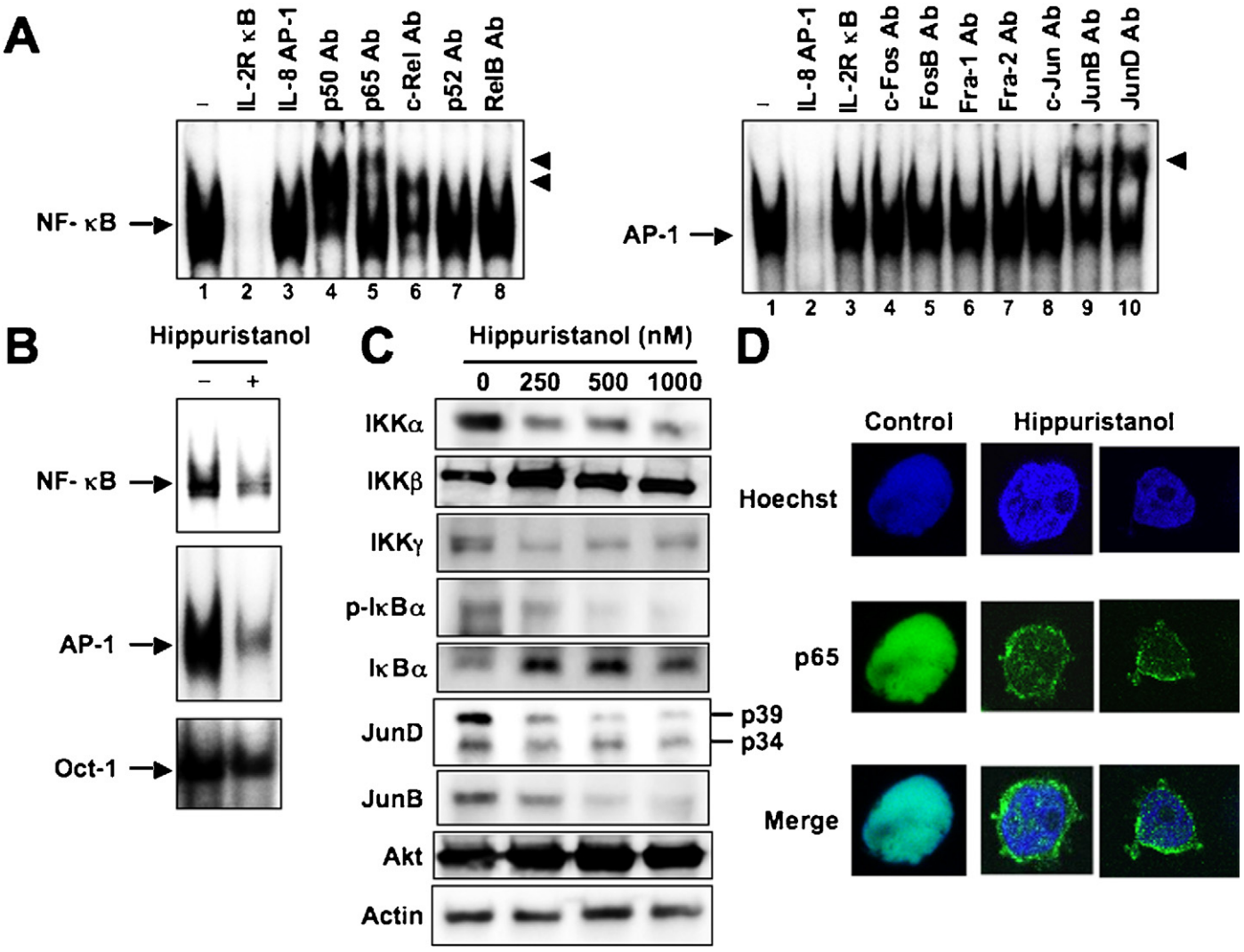

Fig. 5. Hippuristanol inhibits NF-kappaB and AP-1 activities in HTLV-1-infected T-cell line. (A) EMSA using untreated HUT-102 nuclear extracts and radiolabeled NF-kappaB and AP-1 probes generated DNA–protein complexes, which were eliminated by 100-fold molar excess of self-competitors but not by the same molar excess of the irrespective oligonucleotides. Supershift assays using the radiolabeled NF-kappaB and AP-1 probes, untreated nuclear extracts, and the indicated antibodies (Ab) to NF-kappaB and AP-1 components showed that the NF-kappaB and AP-1 bands consisted of p50, p65 and c-Rel subunits and JunB and JunD subunits, respectively. Arrows indicate the specific complexes, while arrowheads indicate the DNA binding complexes supershifted by antibodies. (B) Effects of hippuristanol on activation of NF-kappaB, AP-1 and Oct-1 in HUT-102 cells assessed by EMSA using oligonucleotide probes for NF-kappaB, AP-1 and Oct-1, respectively. Cells were treated with 1000 nM hippuristanol for 24 h. (C) Effects of hippuristanol on the levels of IKK, IkappaBalpha, AP-1 subunits, and phosphorylated IkappaBalpha by Western blot analysis. Cells were treated with various concentrations of hippuristanol for 24 h, followed by protein extraction. Whole cell extracts of treated cells were immunoblotted with specific antibodies. (D) Inhibition of nuclear translocation of NF-kappaB p65 by hippuristanol. Representative results of immunofluorescence analyses in HUT-102 cells treated with 1000 nM hippuristanol for 12 h using antibody against NF-kappaB p65. Original magnification, 1000×.

HUT-102 cells. NF-kappaB oligonucleotide probe with nuclear extracts from untreated HUT-102 cells generated DNA–protein gel shift complexes (Fig. 5A, left). These complexes were due to specific bindings of nuclear proteins to the NF-kappaB sequences because the binding activities were reduced by the addition of cold probe but not by an irrespective sequence (Fig. 5A, left, lanes 2 and 3). The results also showed that NF–kappaB complexes contain p50, p65 and c-Rel in HUT-102 cells (Fig. 5A, left, lanes 4–6). As shown in Fig. 5B, treatment of nuclear extracts prepared from HUT-102 cells with hippuristanol reduced the intensity of the NF-kappaB-containing gel shift complexes, suggesting that hippuristanol down-regulates the DNA-binding activities of NF-kappaB. Inhibition appeared specific to NF-kappaB and was not due to cell death because no significant change in binding activity of Oct-1 was observed after treatment of cells with hippuristanol (Fig. 5B).

Degradation of IkappaBalpha and subsequent release of NF-kappaB require prior phosphorylation at Ser32 and Ser36 residues [27]. To investigate whether the inhibitory effects of hippuristanol are mediated through alteration of phosphorylation of IkappaBalpha, HUT-102 cells were treated with hippuristanol and their protein extracts were checked for phospho-IkappaBalpha expression. Untreated cells constitutively expressed Ser32- and Ser36-phosphorylated IkappaBalpha (Fig. 5C), while hippuristanol decreased the levels of phosphorylated IkappaBalpha, with a concomitant rise in IkappaBalpha level. Phosphorylation of IkappaBalpha is initiated by activated IKK. The IKK complex contains two highly homologous kinase subunits, IKKalpha and IKKbeta, and a regulatory subunit IKKgamma [27]. Hippuristanol inhibited IKKalpha and IKKgamma expression, but not IKKbeta and Akt expression, suggesting that hippuristanol suppresses NF-kappaB activation by inhibiting IKKalpha and IKKgamma expression (Fig. 5C). We next examined the effect of hippuristanol on the cellular distribution of NF-kappaB components using fluorescence microscopy. Hippuristanol blocked nuclear localization of NF-kappaB p65 in HUT-102 cells, which constitutively express this protein in the cell nucleus in the absence of hippuristanol (Fig. 5D).

3.8. Inhibitory effects of hippuristanol on AP-1 activation

AP-1 is also a crucial mediator of both cell cycle promoting and cell-death inhibiting pathways in HTLV-1-infected T cells [6]. Therefore, we examined the effect of hippuristanol on AP-1. High constitutive AP-1 DNA-binding activities were detected in HUT-102 cells (Fig. 5A, right). Supershift analysis with antibodies indicated that the AP-1 complex in HUT-102 cells contained JunB and JunD (Fig. 5A, right, lanes 9 and 10). As shown in Fig. 5B, AP-1 DNA-binding activity diminished in the presence of hippuristanol. In addition, hippuristanol also dose-dependently decreased the expression of JunB and JunD (Fig. 5C). These findings suggest that hippuristanol depletes JunB and JunD, resulting in inactivation of AP-1.

3.9. Hippuristanol suppresses the expression of CA II in HTLV-1-infected T cells

CA catalyzes the hydration of CO_2 to bicarbonate. Bicarbonate is an important substrate for many fundamental biological pathways

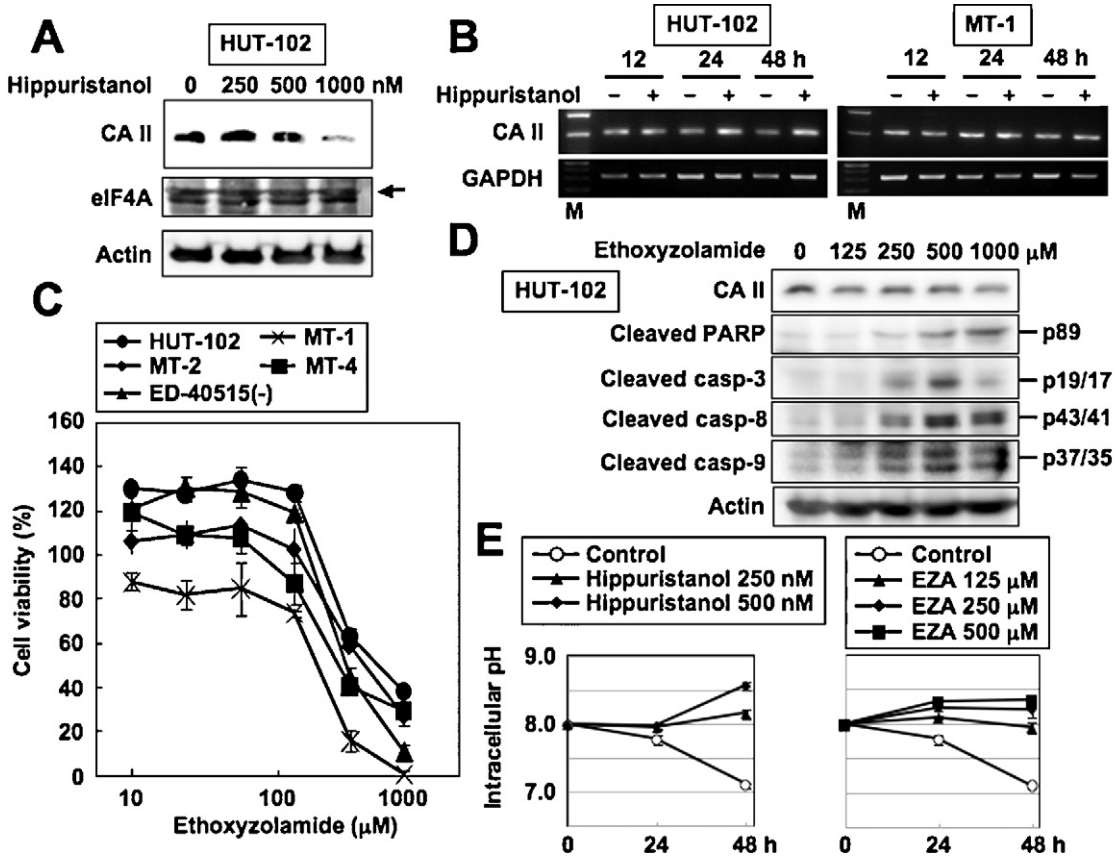

Fig. 6. Hippuristanol suppresses CA II. (A) Hippuristanol suppresses the expression of CA II protein. Western blot of CA II and eIF4A from HUT-102 cells treated with various concentrations of hippuristanol for 24 h. (B) HUT-102 and MT-1 cells were treated with or without 1000 nM hippuristanol for the indicated time periods, and CA II mRNA was detected by RT-PCR. Lane M, molecular mass marker. (C) Ethoxyzolamide inhibits cell viability. HTLV-1-infected T-cell lines were incubated with various concentrations of ethoxyzolamide for 48 h. Then, its effect on cell viability was determined in triplicate cultures by WST-8 assay. The results are expressed as percentage of control and represent mean ± SD of the results obtained. (D) HUT-102 cells were incubated with various concentrations of ethoxyzolamide for 48 h. Caspase activity was detected by cleavage of PARP, caspase-3, -8 and -9 by immunoblot analysis. (E) Effects of hippuristanol or ethoxyzolamide on intracellular pH in HUT-102 cells. Treatment with the indicated concentrations of hippuristanol or ethoxyzolamide (EZA) elevated intracellular pH levels. The results represent mean ± SD of the results obtained.

such as gluconeogenesis, lipogenesis, ureagenesis, pyrimidine synthesis and synthesis of several amino acids [28]. Cancer cells have a higher replication rate than normal cells requiring a high flux of bicarbonate into these metabolic pathways. Therefore, providing as substrate, CA isoforms seem to play an important role in tumor cell growth. Programmed cell death 4 (Pdcd4) protein, a novel tumor suppressor, directly interacts with eIF4A and inhibits protein synthesis by interfering with the assembly of the cap-dependent translation initiation complex [29]. 2-D-electrophoresis showed that pdcd4 suppresses CA II expression [29]. Because hippuristanol also interacts with eIF4A [8], we tested whether hippuristanol inhibits CA II expression in HTLV-1-infected T-cell lines. Western blot analysis showed reduction of expression of CA II, but not eIF4A in HUT-102 cells treated with hippuristanol in a dose-dependent manner (Fig. 6A). However, hippuristanol did not inhibit CA II mRNA expression (Fig. 6B), suggesting that hippuristanol inhibits translation of CA II mRNA.

Since suppression of CA II by hippuristanol inhibits cell growth of HTLV-1-infected T-cell lines, inhibitors of CA might exert similar effects. To test this assumption, HTLV-1-infected T-cell lines were incubated with various concentrations of ethoxyzolamide. As shown in Fig. 6C, in all 5 cell lines, ethoxyzolamide concentration-dependently inhibited cell viability. We next investigated the involvement of caspases in ethoxyzolamide-induced suppression of cell viability by measuring the cleavage of caspase substrates. Immunoblot analysis showed that PARP, caspase-3, -8 and -9 were processed in HUT-102 cells treated with ethoxyzolamide in a dose-dependent manner (Fig. 6D).

CA catalyzes the reversible hydration-dehydration of CO_2, speeding up the formation of H^+ and HCO_3^- in many tissues [30]. Treatment with ethoxyzolamide or CA II-antisense oligonucleotide elevated intracellular pH in ameloblasts [31]. Therefore, intracellular pH in HUT-102 cells was measured by BCECF-AM staining, and the results indicated that the intracellular pH decreased during culture. Treatment with hippuristanol or ethoxyzolamide reversed this pH change, with intracellular pH increasing in a dose-dependent manner (Fig. 6E). These results suggest that suppression of CA II, at least in part, may be responsible for the effects of hippuristanol on HUT-102 cells.

3.10. In vivo effects of hippuristanol on SCID mice inoculated with HTLV-1-infected T-cell line

Is hippuristanol effective against ATL based on its *in vitro* suppression of ATL cell viability? To answer this question, we examined the *in vivo* effects of hippuristanol in a SCID mouse model. After 28-day treatment, the mean tumor volume (Fig. 7A) and weight (Fig. 7B) were significantly lower than those of untreated mice. There was no significant difference in body weight gain between day 0 and 28 among the untreated and treated groups (Fig. 7C). During the same period, mice treated with hippuristanol appeared generally healthy. Treatment with hippuristanol for 28 days in HUT-102 cells produced intensive HE staining indicating apoptosis (Fig. 7D). TUNEL assay showed few apoptotic cells in tumors from untreated mice, while abundant apoptotic cells were noted in tumors from hippuristanol-treated mice

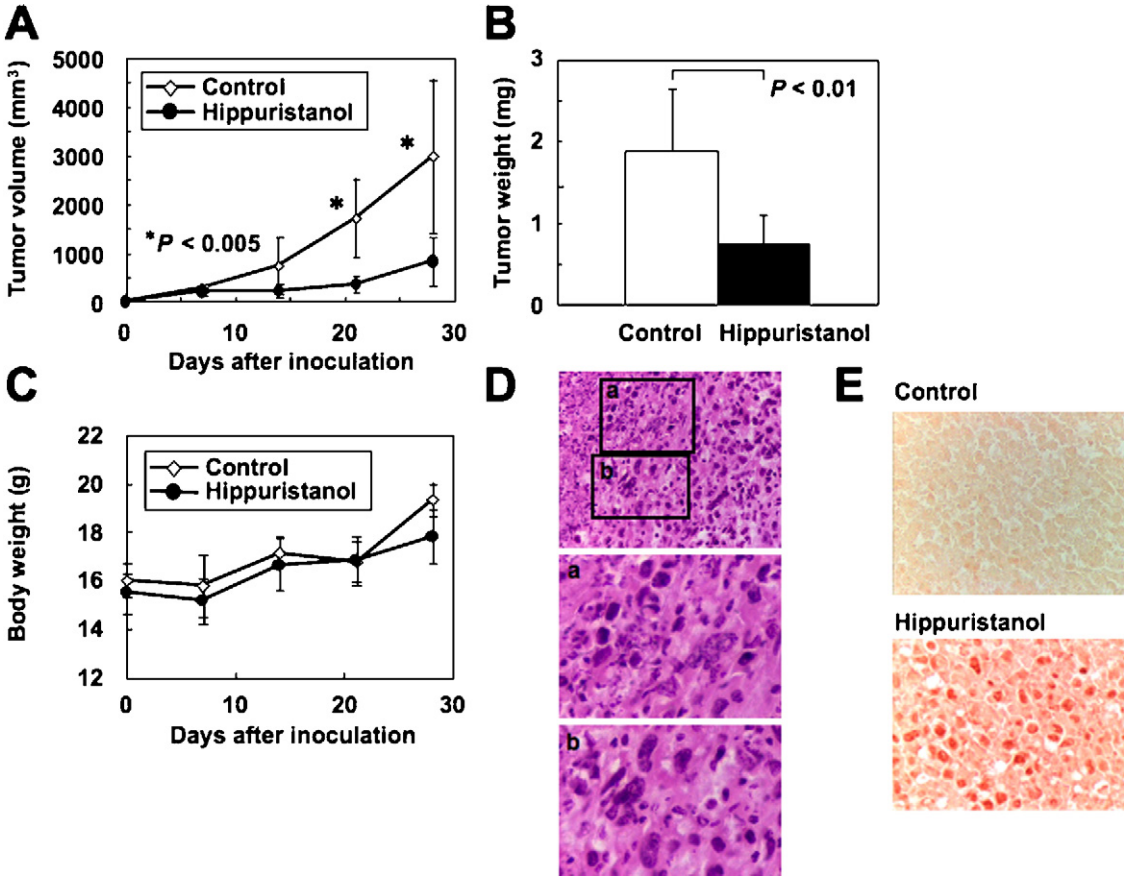

Fig. 7. Inhibition of growth of HUT-102 cells in SCID mice. (A) Growth of the tumors after inoculation of HUT-102 cells subcutaneously. The mice were monitored for tumor volumes. (B) Weight of tumors removed from hippuristanol-treated mice and untreated mice at day 28 after cell inoculation. (C) Body weight of mice was measured weekly for 4 weeks. Data are expressed as mean ± SD of six mice in each group. (D) Pathological changes in HUT-102 tumor cells in the treatment group were evaluated using HE. Magnification, 400× (top). Middle and bottom panels show higher magnification in (a) and (b) areas, respectively. (E) TUNEL assays show apoptotic cells in tumors from mice treated with or without hippuristanol. Note the presence of few apoptotic cells in tumors from the untreated mice (top), compared with the abundant apoptotic cells in tumors from the hippuristanol-treated mice (bottom). Magnification, 400×.

(Fig. 7E). These results suggest that hippuristanol has anti-ATL effects *in vivo*.

4. Discussion

The mRNA binding translation factors (eIF4s) selectively modulate the translation of different mRNAs based on their differing properties, especially the extent of inhibitory secondary structure in their 5′ untranslated regions. The mRNA 5′ cap is recognized by eIF4E, which can then recruit other translation factors including the helicase eIF4A [32]. There are two highly related eIF4A gene products, eIF4AI and eIF4AII. Hippuristanol interacts with the eIF4AI-carboxy-terminal domain and blocks the RNA-dependent ATPase, RNA binding and helicase activities of eIF4AI, hence inhibiting translational initiation [8]. Translational control plays a key role in regulating cell growth. Furthermore, translation is also necessary for viral infection. We found high levels of constitutively expressed eIF4A in HTLV-1-infected T-cell lines. In the next series of experiments, we investigated the anti-ATL effects of hippuristanol.

Hippuristanol demonstrated selectivity in suppression of cell viability of all HTLV-1-infected T-cell lines as well as primary ATL cells, with minimal suppression in normal PBMC. The viral Tax protein plays a critical role in the regulation of proliferation and transformation of HTLV-1-infected T cells during the preleukemic stages. On the other hand, HBZ, encoded on the antisense strand of the proviral DNA, is involved in the transformation of infected cells into malignant cells [25]. However, hippuristanol did not inhibit the expression of viral Tax protein and HBZ mRNA in HUT-102 cells. These results imply that hippuristanol does not effectively inhibit viral replication. Consequently, we studied the mechanism of hippuristanol-induced inhibition of cell viability in HTLV-1-infected T cells.

Our results suggest that hippuristanol induces cell cycle G_1 phase arrest in HTLV-1-infected T-cell lines. Western blot analysis indicates that down-regulation of the key regulators of the G_1/S transition such as cyclin D1, cyclin D2, CDK4 and CDK6, seems to play an important role in hippuristanol-induced cell cycle arrest. We demonstrated that apoptosis is the major mechanism of hippuristanol-induced HTLV-1-infected T cell death, evidenced by increased nuclear fragmentation as well as 7A6. Furthermore, analysis of the apoptotic pathway identified activation of both membrane and mitochondrial pathways, as evidenced by activation of caspase-8 and -9. Hippuristanol down-regulated the expression of anti-apoptotic proteins, Bcl-x_L, c-IAP2 and XIAP. Bcl-x_L is the principal regulator of the mitochondrial-dependent pathway for apoptosis [33], and its down-regulation is involved in caspase-9-dependent apoptosis. Because c-IAP2 and XIAP are associated with caspase-3 and caspase-9, which inhibit their activities [34], it appears that hippuristanol stimulates caspase-3- and caspase-9-dependent apoptosis by down-regulating the expression of these IAP family proteins. The anti-apoptotic protein c-FLIP is also known to suppress the activation of caspase-8 [35]. Down-regulation of c-FLIP may be responsible for the hippuristanol-induced caspase-8 activation.

Although it has been considered that hippuristanol-induced down-regulation of cell cycle and apoptosis regulatory proteins depends on direct inhibition of translation, we asked the question; does hippuristanol inhibit NF-kappaB and AP-1 pathways in HTLV-1-infected T cells? NF-kappaB is a transcription factor involved in cell proliferation and apoptosis, and NF-kappaB-mediated cell proliferation and survival are closely related to its downstream genes involved in the cell cycle machinery and suppression of apoptosis [26]. The activated IKK complex containing IKKalpha/IKKbeta/IKKgamma phosphorylates IkappaBalpha. The phosphorylated IkappaBalpha is then ubiquitinated and degraded, which allows transmigration of NF-kappaB from the cytoplasm to the nucleus where it regulates the expression of various genes [27]. In HTLV-1-infected T cells, NF-kappaB activation serves as a proliferative and survival signal [7]. Our EMSA studies indicated that treatment with hippuristanol inhibited NF-kappaB activation. We showed that hippuristanol inhibited phosphorylation of IkappaBalpha and depleted IKKalpha and IKKgamma. Cyclin D2, CDK4, CDK6, Bcl-x_L, c-IAP2, XIAP and c-FLIP genes are regulated by NF-kappaB [18–23]. Therefore, we speculate that hippuristanol suppresses IKKalpha and IKKgamma, and blocks the NF-kappaB signaling pathway, the cell proliferation and survival pathways, to induce cell cycle arrest and apoptosis.

AP-1 is also known to regulate cell proliferation and survival [36], and required for proliferation of HTLV-1-infected T cells [6]. The present study also demonstrated the inhibitory effects of hippuristanol on JunB and JunD expression, resulting in the suppression of AP-1 DNA-binding in HTLV-1-infected T-cell lines. AP-1 regulates the expression and function of cell cycle regulators such as cyclin D1 [37]. In addition, the cyclin D2 promoter contains NF-kappaB and AP-1 sites [38]. It is therefore likely that NF-kappaB and AP-1, in concert, support proliferation of HTLV-1-infected T cells by activating cyclin D1 and cyclin D2. We speculate that hippuristanol inhibits cyclin D1 and cyclin D2 expression through the suppression of both NF-kappaB and AP-1, resulting in the induction of G_1 cell cycle arrest.

CA II was identified as a protein that can be suppressed by pdcd4, an eIF4A inhibitor [29]. In experiments with HUT-102 cells, CA II was also suppressed by hippuristanol, but hippuristanol did not alter CA II mRNA expression, indicating that hippuristanol regulates CA II expression only at the translational level. CA catalyzes the hydration of CO_2 to bicarbonate, which is an important substrate for several metabolic pathways. Since tumor cells grow faster than normal cells, they require a high flux of bicarbonate [28]. Furthermore, suppression of CA may impair tumor cells to eliminate toxic CO_2, which may cause changes in intracellular pH and ion balance and result in cell growth inhibition. Since suppression of CA II by hippuristanol correlated with the inhibition of survival of HTLV-1-infected T-cells, the CA inhibitor ethoxyzolamide was expected to exert a comparable effect. Ethoxyzolamide concentration-dependently inhibited the viability of all tested HTLV-1-infected T-cells, though it did not inhibit NF-kappaB and AP-1 pathways (data not shown). We also found that hippuristanol or ethoxyzolamide increased intracellular pH in HTLV-1-infected T-cells. Hence, we propose that CA II is also a target of hippuristanol, whose function is achieved by decreasing intracellular pH.

In ATL-xenografted mice, hippuristanol suppressed the growth of transplanted cells, in contrast to the significant increase in tumor size observed in untreated mice. Furthermore, apoptotic cells were present in tumors from hippuristanol-treated mice, suggesting that hippuristanol is a potentially suitable therapeutic agent against ATL. Considered together, the inhibitory effects of hippuristanol on both NF-kappaB and AP-1 pathways as well as CA II in HTLV-1-infected cells hold promising leads in treatment of ATL.

Acknowledgments

We acknowledge Dr. Shigeki Sawada and Mr. Keita Tamaki for the expert technical assistance; Drs. Taeko Okudaira, Jun-nosuke Uchihara, Naoya Taira and Kazuiku Ohshiro for providing patient samples; and Dr. Yuetsu Tanaka for providing Tax antibody. We also thank the Fujisaki Cell Center, Hayashibara Biochemical Laboratories for providing HUT-102 and MT-1; and Dr. Michiyuki Maeda for providing the ED-40515(−) cell line.

References

[1] Poiesz BJ, Ruscetti FW, Gazdar AF, Bunn PA, Minna JD, Gallo RC. Detection and isolation of type C retrovirus particles from fresh and cultured lymphocytes of a patient with cutaneous T-cell lymphoma. Proc Natl Acad Sci USA 1980;77:7415–9.

[2] Hinuma Y, Nagata K, Hanaoka M, Nakai M, Matsumoto T, Kinoshita KI, et al. Adult T-cell leukemia: antigen in an ATL cell line and detection of antibodies to the antigen in human sera. Proc Natl Acad Sci USA 1981;78:6476–80.

[3] Yoshida M, Miyoshi I, Hinuma Y. Isolation and characterization of retrovirus from cell lines of human adult T-cell leukemia and its implication in the disease. Proc Natl Acad Sci USA 1982;79:2031–5.

[4] Tobinai K. Current management of adult T-cell leukemia/lymphoma. Oncology 2009;23:1250–6.

[5] Yamada Y, Tomonaga M, Fukuda H, Hanada S, Utsunomiya A, Tara M, et al. A new G-CSF-supported combination chemotherapy, LSG15, for adult T-cell leukaemia-lymphoma: Japan Clinical Oncology Group Study 9303. Br J Haematol 2001;113:375–82.

[6] Hall WW, Fujii M. Deregulation of cell-signaling pathways in HTLV-1 infection. Oncogene 2005;24:5965–75.

[7] Sun S-C, Yamaoka S. Activation of NF-kappaB by HTLV-I and implications for cell transformation. Oncogene 2005;24:5952–64.

[8] Bordeleau M-E, Mori A, Oberer M, Lindqvist L, Chard LS, Higa T, et al. Functional characterization of IRESes by an inhibitor of the RNA helicase eIF4A. Nat Chem Biol 2006;2:213–20.

[9] Arima N, Daitoku Y, Yamamoto Y, Fujimoto K, Ohgaki S, Kojima K, et al. Heterogeneity in response to interleukin 2 and interleukin 2-producing ability of adult T cell leukemia cells. J Immunol 1987;138:3069–74.

[10] Tanaka Y, Yoshida A, Takayama Y, Tsujimoto H, Tsujimoto A, Hayami M, et al. Heterogeneity of antigen molecules recognized by anti-tax1 monoclonal antibody Lt-4 in cell lines bearing human T cell leukemia virus type I and related retroviruses. Jpn J Cancer Res 1990;81:225–31.

[11] Miyoshi I, Kubonishi I, Yoshimoto S, Akagi T, Ohtsuki Y, Shiraishi Y, et al. Type C virus particles in a cord T-cell line derived by co-cultivating normal human cord leukocytes and human leukaemic T cells. Nature 1981;294:770–1.

[12] Yamamoto N, Okada M, Koyanagi Y, Kannagi M, Hinuma Y. Transformation of human leukocytes by cocultivation with an adult T cell leukemia virus producer cell line. Science 1982;217:737–9.

[13] Miyoshi I, Kubonishi I, Sumida M, Hiraki S, Tsubota T, Kimura I, et al. A novel T-cell line derived from adult T-cell leukemia. Gann 1980;71:155–6.

[14] Maeda M, Shimizu A, Ikuta K, Okamoto H, Kashihara M, Uchiyama T, et al. Origin of human T-lymphotrophic virus I-positive T cell lines in adult T cell leukemia. Analysis of T cell receptor gene rearrangement. J Exp Med 1985;162:2169–74.

[15] Zhang C, Ao Z, Seth A, Schlossman SF. A mitochondrial membrane protein defined by a novel monoclonal antibody is preferentially detected in apoptotic cells. J Immunol 1996;157:3980–7.

[16] Antalis TM, Goldbolt D. Isolation nuclei from hematopoietic cell types. Nucl Acids Res 1991;19:4301.

[17] Mori N, Prager D. Transactivation of the interleukin-1alpha promoter by human T-cell leukemia virus type I and type II Tax proteins. Blood 1996;87:3410–7.

[18] Kawakami A, Nakashima T, Sakai H, Urayama S, Yamasaki S, Hida A, et al. Inhibition of caspase cascade by HTLV-I tax through induction of NF-kappaB nuclear translocation. Blood 1999;94:3847–54.

[19] Nicot C, Mahieux R, Takemoto S, Franchini G. Bcl-X_L is up-regulated by HTLV-I and HTLV-II in vitro and in ex vivo ATLL samples. Blood 2000;96:275–81.

[20] Huang Y, Ohtani K, Iwanaga R, Matsumura Y, Nakamura M. Direct transactivation of the human cyclin D2 gene by the oncogene product Tax of human T-cell leukemia virus type I. Oncogene 2001;20:1094–102.

[21] Iwanaga R, Ohtani K, Hayashi T, Nakamura M. Molecular mechanism of cell cycle progression induced by the oncogene product Tax of human T-cell leukemia virus type I. Oncogene 2001;20:2055–67.

[22] Krueger A, Fas SC, Giaisi M, Bleumink M, Merling A, Stumpf C, et al. HTLV-1 Tax protects against CD95-mediated apoptosis by induction of the cellular FLICE-inhibitory protein (c-FLIP). Blood 2006;107:3933–9.

[23] Wäldele K, Silbermann K, Schneider G, Ruckes T, Cullen BR, Grassmann R. Requirement of the human T-cell leukemia virus (HTLV-1) tax-stimulated *HIAP-1* gene for the survival of transformed lymphocytes. Blood 2006;107:4491–9.

[24] Kim Y-M, Geiger TR, Egan DI, Sharma N, Nyborg JK. The HTLV-1 tax protein cooperates with phosphorylated CREB, TORC2 and p300 to activate CRE-dependent cyclin D1 transcription. Oncogene 2010;29:2142–52.

[25] Matsuoka M, Green PL. The HBZ gene, a key player in HTLV-1 pathogenesis. Retrovirology 2009;6:71.

[26] Dolcet X, Llobet D, Pallares J, Matias-Guiu X. NF-kappaB in development and progression of human cancer. Virchows Arch 2005;446:475–82.

[27] Hayden MS, Ghosh S. Shared principles in NF-kappaB signaling. Cell 2008;132:344–62.

[28] Chegwidden WR, Dodgson SJ, Spencer IM. The roles of carbonic anhydrase in metabolism, cell growth and cancer in animals. EXS 2000;90:343–63.

[29] Lankat-Buttgereit B, Gregel C, Knolle A, Hasilik A, Arnold R, Göke R. Pdcd4 inhibits growth of tumor cells by suppression of carbonic anhydrase type II. Mol Cell Endocrinol 2004;214:149–53.

[30] Wagner CA, Geibel JP. Acid–base transport in the collecting duct. J Nephrol 2002;15:S112–27.

[31] Wang X, Suzawa T, Ohtsuka H, Zhao B, Miyamoto Y, Miyauchi T, et al. Carbonic anhydrase II regulates differentiation of ameloblasts via intracellular pH-dependent JNK signaling pathway. J Cell Physiol 2010;225:709–19.

[32] Flynn A, Proud CG. The role of eIF4 in cell proliferation. Cancer Surviv 1996;27:293–310.

[33] Kroemer G, Reed JC. Mitochondrial control of cell death. Nat Med 2000;6:513–9.

[34] Deveraux QL, Roy N, Stennicke HR, Van Arsdale T, Zhou Q, Srinivasula SM, et al. IAPs block apoptotic events induced by caspase-8 and cytochrome *c* by direct inhibition of distinct caspases. EMBO J 1998;17:2215–23.

[35] Thome M, Tschopp J. Regulation of lymphocyte proliferation and death by FLIP. Nat Rev Immunol 2001;1:50–8.

[36] Hess J, Angel P, Schorpp-Kistner M. AP-1 subunits: quarrel and harmony among siblings. J Cell Sci 2004;117:5965–73.

[37] Shaulian E, Karin M. AP-1 in cell proliferation and survival. Oncogene 2001;20:2390–400.

[38] Brooks AR, Shiffman D, Chan CS, Brooks EE, Milner PG. Functional analysis of the human cyclin D2 and cyclin D3 promoters. J Biol Chem 1996;271:9090–9.